To appear in the Publications of the Astronomical Society of the Pacific - July 2003

The Automated Plate Scanner Catalog of the Palomar Sky Survey. II. The Archived Database

Juan E. Cabanela[1], Roberta M. Humphreys, Greg Aldering[2], Jeffrey A. Larsen[3], Stephen C. Odewahn[4], Peter M. Thurmes[5], and Chris S. Cornuelle

Astronomy Department, University of Minnesota, Minneapolis, MN 55455

juan@aps.umn.edu, roberta@aps.umn.edu

ABSTRACT

The Minnesota Automated Plate Scanner Catalog of the POSS I has been available on-line since 1994. We are now archiving it for distribution to the national and international data centers. In this brief paper we describe the calibration of the digitized data and the characteristics of the archived database.

Subject headings: astronomical databases – catalogs

1. The MAPS Catalog of the POSS I

The Minnesota Automated Plate Scanner (MAPS) Catalog of the first epoch Palomar Sky Survey (POSS I) is derived from our digitized scans of glass copies of the blue(O) and red(E) plates of the original Palomar Observatory Sky Survey for the 632 fields with Galactic latitudes $|b| > 20°$. The scans are done in threshold densitometry mode, recording all pixels above the scanning threshold. The operation of the Automated Plate Scanner (APS) and the scanning procedures are described in detail in Pennington *et al.* (1993), hereafter Paper I. The MAPS Catalog of the POSS I (hereafter simply referred to as "the Catalog") contains coordinates, magnitudes, colors, and several other computed image parameters for all of the matched images on the blue and red plates for nearly 90 million stars and galaxies down to fainter than 21^{st} magnitude (in the blue).

---

[1]Now at Haverford College

[2]Now at Lawrence Berkeley Laboratory

[3]Now at Lunar and Planetary Laboratory, University of Arizona

[4]Now at Arizona State University

[5]Now at Honeywell Inc., Minneapolis, MN

The stellar and non-stellar images are separated using a neural network image classifier Odewahn *et al.* (1992, 1993), that has been trained to the plate limit. The Catalog of objects is available at the APS website (`http://aps.umn.edu/`). The pixel data have also been archived and include all of the matched images in the Catalog of objects, as well as the unmatched images above the noise threshold.

The Catalog has been on-line at the APS website since 1994 and has been the source of basic data for numerous research programs in Galactic and extragalactic astronomy. Using APS galaxy classification and appropriately chosen photometric and morphological parameters from the APS data, Odewahn & Aldering (1995) mapped high density filamentary structure and clustering at the North Galactic Pole, a region covering 389 square degrees on the sky. Cabanela (1999) used a diameter–limited sample of 217,768 galaxies from 96 POSS I fields within 30° of the NGP (the MAPS-NGP catalog) for a comprehensive study of galaxy properties[6]. The Catalog has also been instrumental in the identification of several hundred low surface brightness galaxies (LSBs) using a selection effect in which LSBs have their POSS I colors driven toward the "blue edge" (Cabanela & Dickey 2002). Cabanela & Roscioli (2003) are currently using this technique to map out the distribution of LSBs relative to previously identified large-scale structure. Using star counts from 88 POSS I fields (2,524,740 stars) Larsen & Humphreys (2003) developed a Galactic model optimized for large all–sky surveys. In a very different application, Gordon *et al.* (1998) used the APS Catalog to remove the stars and galaxies from measurements by the Imaging Photo-polarimeter on Pioneer 10/11 to measure the extended red emission in the diffuse interstellar medium. With very accurate positions and magnitudes, the APS Catalog is also ideal for cross-identification with other surveys and was used to identify over 30,000 optical counterparts to over a quarter million point sources from the FIRST radio survey (White *et al.* 2000).

Until now, the Catalog has only existed in the form of a proprietary database available through the APS website. We have now finished archiving the Catalog into easily readable binary files for distribution to the national and international data centers. In this paper we provide a description of the calibration, a summary of the object classification and the characteristics of the final archived database.

2. The Digitized Data and Its Calibration

The scanning procedures and the initial processing of the raw data from the scanner, image reconstruction, flat-fielding and gain correction and plate-to-plate alignment are described in Paper I.

[6]A digital version of this MAPS-NGP catalog is available at the APS website, SIMBAD, and NED.

2.1. Astrometry

The APS is a high precision measuring machine capable of producing very accurate position measurements. It has a repeatability of 1.6μm in x and 0.9μm in y, corresponding to $0\farcs11$ and $0\farcs06$, respectively. However, the final accuracy of any astrometry also depends on the quality of the plates, the centroiding algorithm, and the accuracy and density of the astrometric reference catalogs used. By examining the regions where plate pairs overlap, as well as the positions on the O and E exposures of a given field, we have established that APS object positions are locally accurate to an rms of $0\farcs2$. Achieving this accuracy over an entire Schmidt plate can be quite difficult. In particular, two basic problems arise when astrometry is attempted on a full Schmidt plate. The bright astrometric standards are badly saturated and are distorted by flare at the plate edges. And second, Schmidt plates suffer from distortions which are especially severe ($\sim1\farcs5$) near their edges (Taff 1989; Taff *et al.* 1990).

APS astrometry is done in three steps which overcome these problems and obtain a good full-plate astrometric solution.

1. *Fitting to the diffraction spikes of bright reference stars.* We determine the centers of reference stars from the Astrographic Catalog of Reference Stars (ACRS; Corbin & Urban (1988, 1989)) using the intersection of the Schmidt diffraction spikes. This has the important advantage that the derived center is not affected by the very obvious flare and distortions of bright images which occurs in the vignetted region outside of the central 5.4° diameter of each plate. We use the image pixels of each reference star from the threshold densitometry data and fit the ridgelines of the spikes which are clearly visible and easily measured for the faintest reference stars in the ACRS. A linear plate model plus a cubic radial term needed to correct for the difference between the gnomonic and Schmidt projects is used. With this initial solution we achieve an internal rms error of $0\farcs5$ to $0\farcs6$ in both dimensions.

2. *Corrections for Schmidt plate distortions.* The positional errors caused by Schmidt plate distortions are sufficiently stable that they can be mapped and removed. By co-adding the astrometric residuals for 50 plates reduced as described above, we have mapped the distortion pattern on the POSS I. Specifically, we have succeeded in fitting it with a relatively simple, axisymmetric analytic function with an rms accuracy of $0\farcs07$ in each coordinate. This is essentially the machine limit. When the corrections are applied to the reference stars the rms error typically decreases to $\sim 0\farcs4$.

3. *Astrometry with faint Lick NPM1 stars.* Most objects in the POSS I Catalog are much too faint ($>$ 12 mag) for diffraction spike centroiding. The Lick Northern Proper Motion (Lick NPM1) Catalog (Klemola *et al.* 1994) contains numerous faint stars (down to 18 mag) on the FK4 system. Tests made using the ACRS-derived distortion map and a simple median centroider on Lick NPM1 stars gives astrometric solutions with rms $\sim 0\farcs25$ per coordinate. Using the Lick NPM1 stars plus the distortion corrections, we obtain full-plate solutions with

an rms of $0\farcs2 - 0\farcs3$ in RA and Declination. The Lick NPM1 ends at Declination $-23°$, so for those POSS I fields with field centers south of this and for any fields for which the Lick data are not available, we use the ACRS which typically yields full-plate rms errors of $\sim 0\farcs4$. The astrometric positions of both the stars and galaxies are then derived from the median centroid of the background subtracted pixel data. Information about the astrometric solution for each POSS field is included with the archived Catalog.

This scheme supposes that the distortion pattern determined from the diffraction spike centroids is generic, and will therefore apply to faint objects on the plates. Since we ultimately calculate the astrometric solution using the NPM1 catalog, with the full catalog in hand, we can test this assumption directly by stacking the residuals of the final catalog according to plate location for all the plate solutions. This procedures applied to 533 plates reveals some systematic residuals of the NPM1 positions at the plate edges, but these were typically less than or comparable to the dispersion in the offsets at a given location across all plates (which reflects the combined effects of random measurement errors for individual objects and the stability of the distortion pattern across all plates). Therefore, we conclude that the distortion model based on the diffraction spikes is adequate and is appropriate for use in calculating the final astrometric solution based on median centroids.

After the above steps have produced an astrometric solution, application of the astrometric solution to the median centroids of the catalog objects provides correct positions for stars fainter than m$\sim$12 and for all galaxies. We caution that due to the aforementioned combination of flaring and saturation of brighter stars, a magnitude-dependent — approximately radial — error in the cataloged positions results when the astrometric solution is then applied to the median centroids of bright stars in the outer vignetted region of the plate. Again, galaxies are not affected in this way because such bright galaxies are well resolved and unsaturated. Likewise, brighter stars in the central $5.4°$ of the plates do not suffer this effect. Although use of the diffraction spike centroids in the main catalog — or application of a magnitude-dependent correction — could remedy this problem, since MAPS emphasizes unsaturated objects we have chosen not to introduce such a dichotomous astrometric scheme.

In order to examine our astrometry for systematic effects, we have compared our positions on 159 POSS I E plates with those of radio sources detected in the FIRST survey (Becker, White, & Helfand 1995). For most plates, the February 1998 version of the FIRST catalog was used. The coordinates were precessed from J2000 FK5 to B1950 FK4 using the IPAC/JPL precession software suite. The distribution of nearest-associations is modeled as a Gaussian core — representing true associations — and a constant background — representing false associations due to interlopers. Our data indicate that for separations of less than 1–2″ the number of true associations overwhelms the number of false associations. Over the entire FIRST catalog we find the Gaussian core to be offset by $-0\farcs018 \pm 0\farcs003$ in Right Ascension and $-0\farcs130 \pm 0\farcs003$ in Declination, in the sense of APS$-$FIRST. The quoted uncertainties on the offsets are purely statistical. The Gaussian core, representing roughly 20,000 APS-FIRST associations, has a dispersion of $0\farcs52$ both in Right Ascension and

Declination, consistent with the stated positional accuracy of $< 1''$ for FIRST, and our measured astrometric residuals of $\sim 0\farcs3$ RMS. As discussed by McMahon, White, Helfand, & Becker (2002) and Ivezić et al. (2002), the majority of optical counterparts detectable on POSS I are resolved galaxies, while some radio sources are themselves extended; both effects will increase the position differences as well as the completeness and reliability of the cross-identifications. However, these issues have little impact on determining the mean astrometric offsets. We also examined whether the above offsets depend on Right Ascension or Declination, but failed to find any convincing trends.

2.2. Photometry – Stars and Galaxies

The photometric calibration for stars uses a magnitude-diameter relation derived from photoelectric BV, BVR$_J$ and CCD BVR$_c$ calibrating sequences. Our CCD sequences were obtained at Capilla Peak Observatory (University of New Mexico), Cerro Tololo Interamerican Observatory and McDonald Observatory, and our photoelectric photometry at Kitt Peak National Observatory (Humphreys *et al.* 1991) . The sequences range from about 13 to 20–21 mag. and are transformed to the instrumental (emulsion + filter system) O and E magnitudes corresponding to the blue and red Sky Survey plates, respectively (Humphreys *et al.* 1991). The color transforms are shown in Figure 1. We supplement our photometry with data for brighter stars from the Guide Star Photometry Catalog (Lasker *et al.* 1988) to give a calibration from ∼10 to 20–21 mag for the O plates. The calibrating sequences are included in the archived database.

The diameters are measured from the best-fit ellipse to the single level of isodensity data. The magnitude-diameter relations for each field are then fit by a smooth curve whose expected shape is derived from the stellar PSF (King 1971; Kormendy 1973). The resulting fits typically have a mean rms of 0.15–0.20 mag over the range 14–20 mag. Sample magnitude–diameter relations are shown in Figure 2. The APS magnitudes are most reliable fainter than 12th mag because of the diffraction pattern, and are not available for objects brighter than 8th magnitude.

Humphreys *et al.* (1991) found that the magnitude-diameter relations for the POSS I fields all have essentially the same form or shape with small zero-point variations. Thus for those fields for which we do not have CCD or photoelectric calibration to the fainter magnitudes, we use the mean relation fit to the brighter stars in the GSPC (BV photometry only). We obtain the necessary R photometry with the CCD camera at the Univ. of Minnesota's O'Brien Observatory or assume that the GSPC stars are main sequence stars and adopt the corresponding V-R$_c$ color. Tests of this method on well-calibrated fields give magnitudes agreeing to within 0.2 mag.

Schmidt plates have a systematic vignetting error across the field. The vignetting correction is a function of the radial distance from the plate center with no correction out to $\approx 2.7°$. We have tested the expected or theoretical vignetting function by a comparison with a grid of CCD frames on two POSS fields, critically placed in the plate corners and along the radial, horizontal

and vertical axes. Our empirically-determined correction (maximum ∼0.3 mag in the plate corners) is consistent with the expected function. The vignetting function is included in the reductions and the corrections are applied to the measured magnitudes where appropriate.

Because galaxy images are extended on the sky, a more elaborate method of photometry than that used in stellar photometry is required. We have developed a set of plate calibration techniques to derive the density-to-intensity transformation properties of each glass copy plate and to set the photometric zero-point based on available stellar photometry. The most fundamental method uses a direct link between APS galaxy luminosity profiles and available high-quality photometric profiles derived from CCD images to establish a simple linear transformation in log(I)-D space, where D is the raw photographic density as measured by the APS. In the absence of available surface photometry, which is the case for most POSS I fields, we adopt a density-to-intensity transformation derived by comparing the mean stellar point spread functions of stars over a wide range in magnitude (Bunclark & Irwin 1984). The profile slope is derived from the bright stars and the zero point is set by the photometric standards. We use the background subtracted pixel data for both the stars and galaxies to derive the integrated magnitude. Due to the small plate scale of the POSS I and the adverse effects of scattered light in the presence of saturated stellar cores, this method is not as effective as the previous one, but it does produce sufficiently reliable results. In addition the stellar PSF technique produces an estimate of the seeing on each plate.

Comparing our O and E band radial surface brightness profiles with three independent sources of galaxy surface photometry, we found no systematic deviation in surface brightness over the ranges $21.0 \leq \mu_O \leq 24.5$ and $20.5 \leq \mu_E \leq 23.5$. The accidental errors associated with the APS surface brightness measurements are in the range $0.07 \leq \sigma_\mu \leq 0.15$ for both the O and E plates. Comparison with available photometry in the RC3 and fainter galaxy catalogs at the NGP show that APS-derived integrated galaxy magnitudes (extrapolated total magnitudes in the case of O$\leq$ 17) show no systematic photometric errors for O$\leq$ 19.5 and a typical rms scatter of 0.2 to 0.3 magnitudes (see Odewahn & Aldering (1995)).

The integrated (magi) and the magnitude–diameter relation (magd) magnitudes are both included in the Catalog for every object. Obviously, magd should be used for stars and magi for galaxies. The advantage of including both for each object occurs if a "star" is later found to be a "galaxy" or vice-versa, then the appropriate magnitude is available.

2.3. Object Classification

We use an artificial neural network (ANN) classifier (Odewahn *et al.* (1992, 1993) and Odewahn (1995)) to classify each image as either a star or a non–stellar image (galaxy) (non-stellar). The images are independently classified on both the O and E plates, but the O-plate classification is preferred and is used in the database because it gives a higher success rate and has shown better repeatability. Our first ANN classifier yielded a success rate above 90% down to 20.0 - 20.5 mag

for stars, and 19.5 mag for galaxies. But for objects fainter than 19.5 – 20th magnitude, it was an extrapolation of networks trained on brighter objects. We now use an ANN trained to the plate limit using fainter known galaxies from the Infante & Pritchet (1992) catalog of galaxies at the NGP. This improved network yields a success rate better than 96% for both stars and galaxies with image diameters greater than $4\farcs9$ or $\sim 21^{st}$ magnitude for the O plate and ∼80% success for smaller images down to our processing limit at about $1\farcs7$. Figure 3 shows the number of stars and galaxies as a function of magnitude for the NGP field P323.

The neural network has two output nodes, one for galaxies and one for stars. The value at each is a measure of the probability that the image is an object of that class, and the sum of the two node values is unity. The "galnode" parameter is the value from the galaxy node and is included in the database. When galnode from the O plate exceeds 0.50, the image is classified as a galaxy. Obviously galnode values near 0.50 indicate that the classification is uncertain. In this two-class system, blended or merged images are almost always classified as galaxies (non-stellar). This can be a problem for fields near the Galactic plane where the density of images is high (see Larsen & Humphreys (2003)).

Based on the ANN classifier, the 89,234,404 objects in the Catalog consist of 56,391,694 "stars" and 32,842,710 non-stellar objects or "galaxies".

2.4. The Database Pipeline

The processed data are placed through an automated database pipeline that applies the astrometric solution, calculates the magnitudes and several other image parameters including the ellipticity to the best fit ellipse, the major–axis position angle, mean surface brightness, image moments, and concentration indices for all of the O and E images. The O and E images are then matched in Right Ascension and Declination using an algorithm that varies the matching radius with the diameter of the image.[7] This results in two separate databases of matched and unmatched images. All of the objects, matched and unmatched, are then classified using the ANN classifier. Most of the unmatched images are scratches, plate defects or barely above the level of the plate noise; thus, only the matched images are included in the Catalog.

3. Archived Catalog Description

The archived version of the MAPS Catalog of the POSS I contains more than 89 million matched objects on the 632 fields. The sky coverage is illustrated Figure 4. Duplicate observations are recorded for any objects that lie on multiple POSS I fields. The archived Catalog is organized

[7]The rare cases of multiple matches are flagged in the archived Catalog.

into 632 binary datafiles, one for each POSS I field with a header describing the POSS I field. The contents of the header is summarized in Table 1 and includes information on the number of objects in the field, the Right Ascension and Declination limits of the field, and the limiting magnitudes and surface brightness for both plates. The astrometric and photometric uncertainties as well as a seeing estimate for both plates from an analysis of the stellar point spread function are also in the header(see 2.2).

This header is followed by a separate record for each object matched on the O and E plates. In addition to position, magnitudes, color and object class, several image parameters from both plates are provided in a simple combined record. The archived Catalog includes parameters that were not available in the previous on-line version. The parameters are listed in Table 2. Along with parameters describing the image (*e.g.* - flux, major-axis diameter, ellipticity, major-axis position angle) there is a unique identifier or "starnum" from the O plate assigned to each object. This identifier can be used to construct a designation for each object in the Catalog with the form "MAPS PFFF-NNNNNNN" where "FFF" is the POSS I field number and "NNNNNNN" is the object's O plate "starnum" (stored as first integer of each object's record) Thus, for example, the MAPS Catalog counterpart for the galaxy UGC 6000 lies on POSS Field P432 and has O starnum 333220, thus an alternate designation for this galaxy is "MAPS P432-333220"[8]. The archived Catalog also includes information on the astrometric solution and photometric calibration (including the standards used) for each POSS I field.

The archived Catalog is available and can be queried at the APS Project website. It can also be downloaded as binary datafiles with sample source code to read the datafiles and additional information about the file formats and sizes. The Catalog also been distributed to the national and international data centers.

In its more than 20 years of operation the APS Project has benefited from the professional and technical expertise of many people especially Dr. Robert Landau, Dr. Frank Ghigo, Dr. Robert Pennington, Mr. Edward Stockwell, Mr. Stan Shankman, Mr. Jeff Meisner and Mr. William Zumach plus the assistance of numerous graduate and undergraduate student programmers, operators, and system administrators including among many others, Jennifer Bash, Fred Berendse, Tina Bird, Claia Bryja, Natalie Frey, Matt Gray, Clayton Hogan, William Ketzebach, Jennifer Parker, Brian Tapia, Dang Vang, and Jennifer Webster. We also thank Dr. Donald Terndrup (CTIO) and Dr. Steve Gregory (Univ. New Mexico) for their assistance with the photometry observations. We are especially grateful to Kyle Cudworth and Yerkes Observatory for the loan of glass copies of POSS I plates when some of ours were damaged. The APS Project has been supported by the NSF, NASA, and the University of Minnesota. The creation of the archived database is supported by NASA's Applied Information Systems Research Program (NAG 5-9407). The APS-FIRST cross-

[8]This follows the guidelines of the IAU Working Group on Designations. The density of objects in this catalog precluded the use of the positional naming system common in other (smaller) catalogs

identification was supported by the NASA ADP program under grant NASA/NAG 5-2980. JEC also acknowledges support from a Small Research Grant from the AAS.

REFERENCES

Becker, R. H., White, R. L., & Helfand, D. J. 1995, ApJ, 450, 559

Bunclark, P. S. & Irwin, M. J. 1984, in *Astronomy with Schmidt-type Telescopes*, Proceedings of IAU Colloquium 78, ed. M. Capaccioli, (Dordrecht, Holland; Boston, D. Reidel), 147

Cabanela, J. E., 1999, "Galaxy Properties from a Diameter Limited Catalog", Doctoral Dissertation, University of Minnesota

Cabanela, J.E. and Dickey, J.M. 2002, AJ, 124, 78

Cabanela, J.E. and Roscioli, M.B. 2003, AJ, in preparation

Corbin, T. E. & Urban, S. E. 1988, in *Mapping the Sky*, Proceedings of IAU Symposium No. 133, ed. S. Debarbat, (Dordrecht; Kluwer Academic Publisher), 287

Corbin, T. E. & Urban, S. E. 1989, in *Inertial Coordinate Systems on the Sky*, Proceedings of IAU Symposium No. 141, 433

Gordon, K. D., Witt, A. N. & Friedmann, B. C., 1998, ApJ, 498. 522

Humphreys, R. M., Landau, R., Ghigo, F. D., Zumach, W. and LaBonte, A. E., 1991, AJ, 102, 395

Infante, L. & Pritchet, C. J, 1992, ApJS, 83, 237

Ivezić, Ž. et al. 2002, AJ, 124, 2364

King, I. R., 1971, PASP, 83, 199

Klemola, A. R., Hanson, R. B. & Jones, B. F., 1994, Lick Northern Proper Motion Program (NPM1) Catalog (see AJ, 94, 501)

Kormendy, J., 1973, AJ, 78, 255

Larsen, J. A. and Humphreys, R. M., 2003, AJ, in press

Lasker, B. M. et. al., 1988, ApJS, 68, 1

McMahon, R. G., White, R. L., Helfand, D. J., & Becker, R. H. 2002, ApJS, 143, 1

Odewahn, S. C., 1995, PASP, 107, 770

Odewahn, S. C. and Aldering, G., 1995, AJ, 110, 2009

Odewahn, S. C., Stockwell, E. B., Pennington, R. L., Humphreys, R. M. and Zumach, W. A., 1992, AJ, 103, 318

Odewahn, S. C., Humphreys, R. M., Aldering, G. and Thurmes, P., 1993, PASP, 105, 1354

Pennington, R. L., Humphreys, R. M., Odewahn, S. C., Zumach, W. and Thurmes, P. M., 1993, PASP, 105, 521

Taff, L. G., 1989, AJ, 98, 1912

Taff, L. G., Lattanzi, M. G. & Bucciarelli, B., 1990, ApJ, 358, 359

White, R. L. et al. 2000, ApJS, 126, 133

Table 1. Parameters in the POSS I Field Headers.

Parameter	Description
Pxxx	APS POSS I Field Number[a]
Emul	Palomar Sky Survey Emulsion Number
Epoch	Date of observation
NOBJ	Number of objects in the field
NSTARS	Number of objects classified star
NGALAX	Number of objects classified galaxy (non-stellar)
ramin,ramax	Minimum and maximum Right Ascension (B1950)
decmin,decmax	Minimum and maximum Declination(1950)
ra_rms,dec_rms	Positional rms in Right Ascension and Declination
Omaglim,Emaglim	Limiting magnitude on the O and E plates
Oseeing,Eseeing	Seeing estimate from the PSF
Omuth,Emuth	Surface brightness limit from the PSF
Omusky,Emusky	Sky surface brightness estimate from PSF
Ocalsrc,Ecalsrc	Photometric calibration sources
Ocalmin,Ocalmax,Ecalmin,Ecalmax	Minimum and Maximum diameters for the calibration
Orms,Erms	Photometric calibration rms for different magnitude ranges

[a]Sometimes called the "modified Luyten plate number". In this numbering system the two fields at the NCP are labeled P1 and P2, and differs by one(+1) from that used by Luyten and in the Guide Star Catalog

Table 2. Object Parameters in the MAPS Catalog of the POSS I.

Parameter	Description
starnumO, starnumE	image raster number
ra, dec	Right Ascension & Declination (B1950.0)
Xsct, Ysct	X & Y centroid positions on the O & E plates
diaO, diaE	Major–Axis Diameter
magiO	Integrated O magnitude
magdO	O magnitude from the magnitude–diameter relation
object class	Object class, star or galaxy, from the O plate ANN
colori	$O - E$ color from the integrated magnitudes
colord	$O - E$ color from the magnitude–diameter relations
mean_sbO, mean_sbE	Mean Surface Brightness
thetaO , thetaE	Major–Axis position angle of the image
ellO, ellE	Ellipticity of the image
galnodO, galnodE	ANN node output for object classification
PsatO, PsatE	Percent saturation of the image
TavgO, TavgE	Average transmittance of the image
TskyO, TskyE	Sky transmittance around the image
ReffO, ReffE	Effective (half-light) radius (r_{50}) of the image
C_{42}O, C_{42}E	C(r_{100}/r_{50}) concentration index
C_{32}O, C_{32}E	C(r_{100}/r_{75}) concentration index
Mir1O , Mir1E	First Moment of the image
Mir2O , Mir2E	Second Moment of the image
flag	Quality flags noting multiple matches and any unreliable data

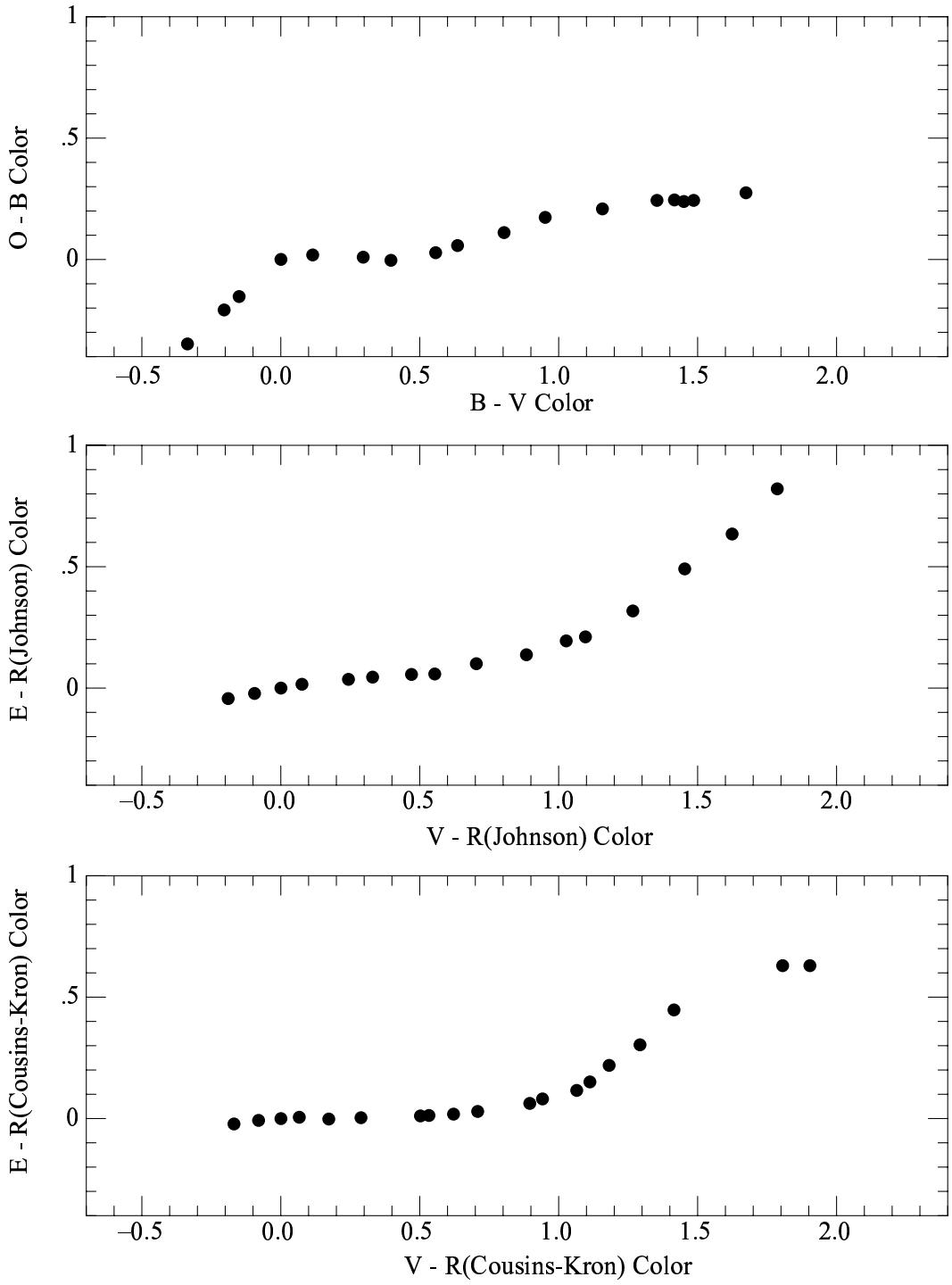

Fig. 1.— Color transformations from the standard BVR photometry to the instrumental O(blue) and E(red) magnitudes of the POSS I

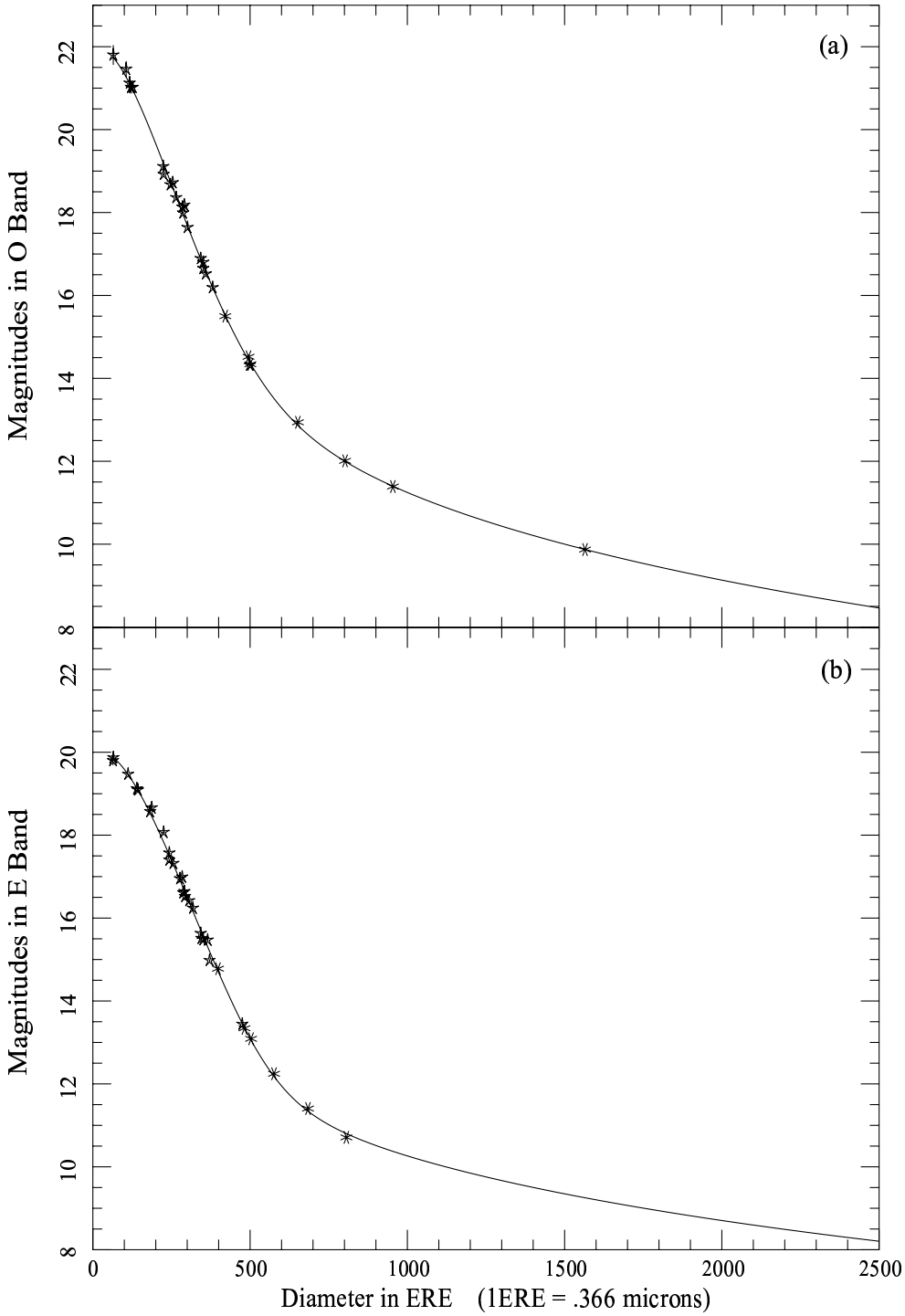

Fig. 2.— Sample magnitude–diameter relations for the O(a) and E(b) plates.

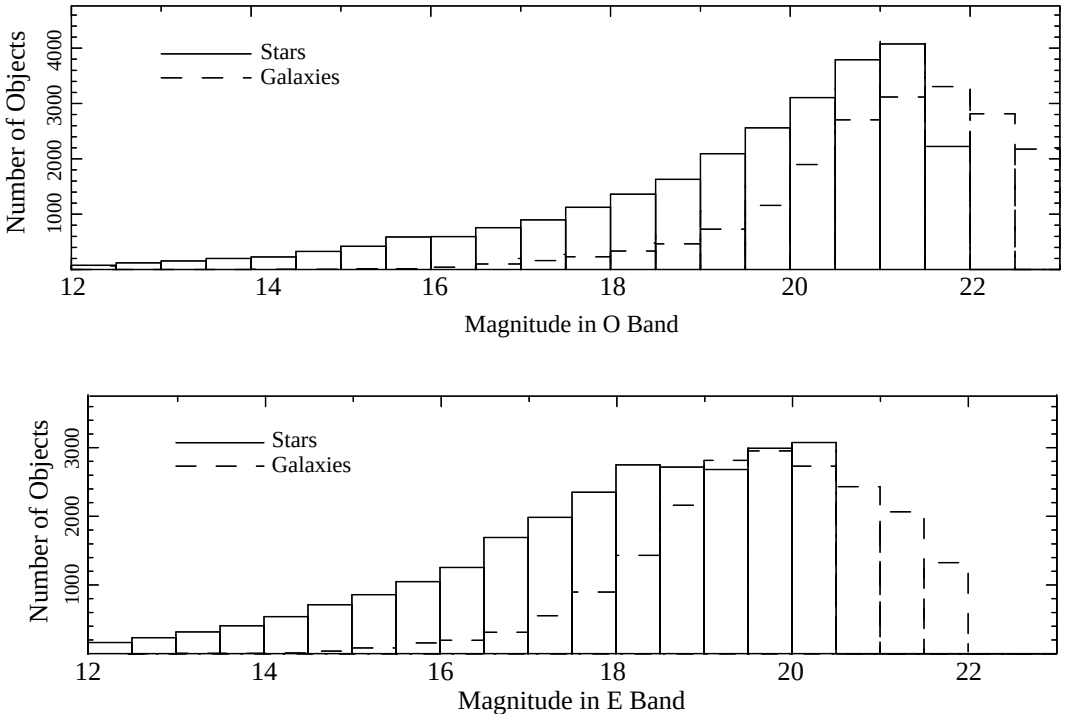

Fig. 3.— The luminosity functions for the stars and galaxies on the P323 O and E plates.

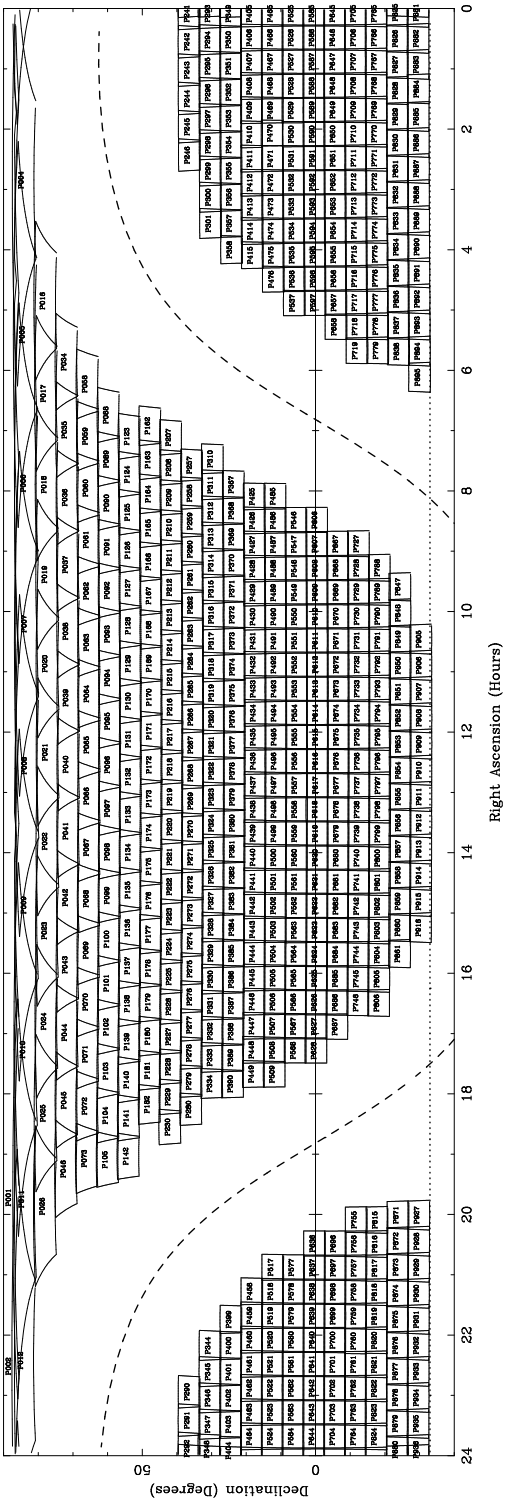

Fig. 4.— Sky coverage of the MAPS Catalog of the POSS I.